



$\text{Fe}^{3+}/\text{Fe}^{2+}$ redox electrolyte for high-performance polyaniline/ SnO_2 supercapacitors

Tian-tian LIU, Yin-hai ZHU, En-hui LIU, Zhen-yu LUO, Tian-tian HU, Zeng-peng LI, Rui DING

Key Laboratory of Environmentally Friendly Chemistry and Applications of Ministry of Education,
College of Chemistry, Xiangtan University, Xiangtan 411105, China

Received 9 October 2014; accepted 30 January 2015

Abstract: The $\text{Fe}^{3+}/\text{Fe}^{2+}$ redox electrolyte for use in polyaniline/tin oxide (PANI/SnO_2) supercapacitors was reported. The influences of redox electrolyte based on different $\text{Fe}^{3+}/\text{Fe}^{2+}$ ion pair concentrations in 1 mol/L H_2SO_4 solution on the pseudocapacitive behaviors of PANI/SnO_2 supercapacitor were investigated. The electrochemical properties of the supercapacitor were studied by cyclic voltammetry (CV), galvanostatic charge–discharge (GCD), and electrochemical impedance spectroscopy (EIS) techniques. It is found that the performance of the supercapacitor is the best when the $\text{Fe}^{3+}/\text{Fe}^{2+}$ concentration is 0.4 mol/L and its initial specific capacitance is 1172 F/g at an applied current density of 1 A/g. The long-term cycling experiment shows good stability with the retention of initial capacitance values of 88% after 2000 galvanostatic cycles. The experimental results testify that using $\text{Fe}^{3+}/\text{Fe}^{2+}$ redox electrolyte has a good prospect for improving the performances of energy-storage devices.

Key words: polyaniline; tin oxide; iron ion; redox electrolyte; supercapacitors

1 Introduction

Electrochemical capacitors (ECs) are currently widely investigated due to their interesting characteristics in terms of high power and energy densities [1–3]. Nowadays, pseudocapacitance materials such as metal oxides and conducting polymers are the most practical materials for supercapacitor electrode [4–6]. Conducting polymer, such as polyaniline (PANI), is one of the most common polymeric materials due to the advantages of easy synthesis, low cost and good conductivity [7,8]. However, the poor stability during the charge/discharge process restricts its practical applications in supercapacitor. To overcome the drawback of PANI, its composites formed with metal oxides, such as SnO_2 , have been widely studied [9,10]. For example, it has been demonstrated that the supercapacitor electrodes based on PANI/SnO_2 have high capacitance and good stability due to the combination of the excellent conducting and mechanical properties of SnO_2 , with high pseudocapacitance of PANI.

Recently, a new and simple redox strategy has been reported. Introducing redox mediators into conventional electrolytes brought enormous capacitive contributions for supercapacitor systems through the reversible Faradic reactions of the redox mediators. ROLDÁN et al [11] reported that the capacitive performance of the supercapacitor in the electrolyte doped by hydroquinone (HQ) can be improved. It was also reported that the specific capacitance of polyaniline/ SnO_2 supercapacitor was 839 F/g at 1 A/g in 1 mol/L H_2SO_4 electrolyte doped by HQ [12]. However, the high toxicity, low solubility and poor electrochemical cyclability of HQ limited its applications. So researching environmental friendly and high-efficient redox mediator is needed which not only keeps the superb properties of PANI/SnO_2 , but also improves the electrochemical performance of supercapacitors based on PANI/SnO_2 materials.

In this study, a redox electrolyte based on different $\text{Fe}^{3+}/\text{Fe}^{2+}$ concentrations in H_2SO_4 solution for use in PANI/SnO_2 supercapacitors is reported. The incorporation of $\text{Fe}^{3+}/\text{Fe}^{2+}$ ion pair into the H_2SO_4 electrolyte leads to great increase of capacitance of PANI/SnO_2 supercapacitors.

2 Experimental

2.1 Electrode material

SnO₂ and PANI/SnO₂ composites were synthesized as previously described [12]. SnO₂ was synthesized based on the hydrothermal route. In a typical synthesis, 2 mmol oxalic acid and 2 mmol cetyltrimethyl ammonium bromide were dissolved in 50 mL deionized water, then, 2 mmol SnCl₂·2H₂O was added to this solution under constant stirring to get a milky solution. The pH value of the resulting solution was adjusted to 9 using dilute NH₃·H₂O solution. Then, the mixed solution was stirred for 2 h at room temperature. Finally, the obtained milky solution was transferred into an 80 mL Teflon-lined stainless steel autoclave. The autoclave was maintained at 150 °C for 10 h and then cooled to room temperature. The final product was collected and washed with distilled water and absolute ethanol for several times, and then was dried in vacuum at 60 °C for 12 h.

The PANI/SnO₂ composites were prepared as follows (the aniline was distilled under reduced pressure before use). 5 mmol oxalic acid was dissolved in 50 mL deionized water. Then, 0.5 mmol SnO₂ and 5 mmol aniline were dispersed in above solution and stirred for 30 min to facilitate aniline to adsorb on the SnO₂. Upon stirring, 5 mmol ammonium persulfate was separately dissolved in 50 mL deionized water and finally added to the above mixture, and the obtained mixture was cooled to 0–5 °C and then kept in a polymerization for 8 h. The resulting powders were filtered and washed successively with water until the filtrate was colourless, and then dried at 50 °C overnight under vacuum.

2.2 Electrolytes

All of the solutions were prepared using analytical grade reagents and used immediately after their preparation. Four different Fe³⁺/Fe²⁺ ion pair concentration redox electrolytes in H₂SO₄ solution, including *n* mol/L [Fe³⁺/Fe²⁺] + 1 mol/L H₂SO₄ (*n*=0.1, 0.3, 0.4, 0.5) were used, the molar ratio of Fe³⁺ and Fe²⁺ was 1:1. For comparison, 1 mol/L solution of H₂SO₄ was also studied. The different valence states of iron ion were obtained from FeSO₄ and Fe₂(SO₄)₃.

2.3 Electrode preparation and electrochemical characterization

The electrode was prepared as following steps. Firstly, 80% (mass fraction) PANI/SnO₂ powder with 10% (mass fraction) acetylene black conductor and 10% (mass fraction) polyvinylidene fluoride emulsion were mixed to form slurry. Then, the slurry was filled into a piece of stainless steel net with a geometric diameter of 10 mm, yielding electrodes with the thickness of 0.2 mm

and the active mass of 3–5 mg. All the electrodes were dried in a vacuum oven at 110 °C overnight before each experiment. Sandwich-type capacitors were constructed with two symmetrical carbon electrodes separated by a nylon septum. The electrochemical testing for supercapacitor was performed on a CHI 660A electrochemical workstation system (CHI Inc., USA) under ambient conditions using two-electrode system. Cyclic voltammetry (CV), galvanostatic charge–discharge (GCD), electrochemical impedance spectroscopy techniques (EIS) and cycle life test were carried out to assess the electrochemical properties of the devices. The CV experiments were performed at varying scan rates. The GCD was conducted with different current densities. The EIS measurements were carried out by applying an AC voltage of 5 mV amplitude in the frequency range of 100 kHz to 10 mHz. The cycling performance was charged and discharged at a constant current density of 1 A/g on a Neware BTS cell test apparatus.

3 Results and discussion

To explore the improvement in capacitive behavior of PANI/SnO₂ supercapacitor induced by Fe³⁺/Fe²⁺ ion pair in H₂SO₄ solution, CV was employed to compare the 1 mol/L H₂SO₄ electrolyte with the *n* mol/L [Fe³⁺/Fe²⁺] + 1 mol/L H₂SO₄ (*n*=0.1, 0.3, 0.4, 0.5) electrolyte at a scan rate of 2 mV/s. The effect of adding Fe³⁺/Fe²⁺ ion pair into the H₂SO₄ electrolyte to the capacitive behavior is clearly observed in Fig. 1. The CV curves obtained in *n* mol/L [Fe³⁺/Fe²⁺] + 1 mol/L H₂SO₄ electrolyte display a couple of relatively broad current peaks with good symmetry that are pseudocapacitive in nature. The CV curve obtained in H₂SO₄ electrolyte shows a quasi-rectangle shape without obvious redox peak. However, the PANI/SnO₂ samples show two pairs of significant redox peaks due to pseudocapacitive behavior of PANI in 1 mol/L H₂SO₄ electrolyte [12]. So the big bumps of CV curves in *n* mol/L [Fe³⁺/Fe²⁺] + 1 mol/L H₂SO₄ electrolyte are associated with the synergistic effects of PANI and Fe³⁺/Fe²⁺. From Fig. 1, it can be seen that when *n* increases from 0.1 to 0.4 mol/L, the redox peak currents increase, while *n* increases from 0.4 to 0.5 mol/L, the redox peak currents decrease. The result clearly indicates that the high concentration of Fe³⁺/Fe²⁺ is favorable for improving the capacitances of the PANI/SnO₂ supercapacitor, but if the Fe³⁺/Fe²⁺ concentration is too high, the ion activity may be reduced due to the less water hydration, resulting in the decrease of ion mobility. The CV area of supercapacitor in 0.4 mol/L [Fe³⁺/Fe²⁺] + 1 mol/L H₂SO₄ electrolytes is the largest, implying the largest specific capacitance value.

To understand the electrochemical nature of this electrode process, the CV tests of PANI/SnO₂

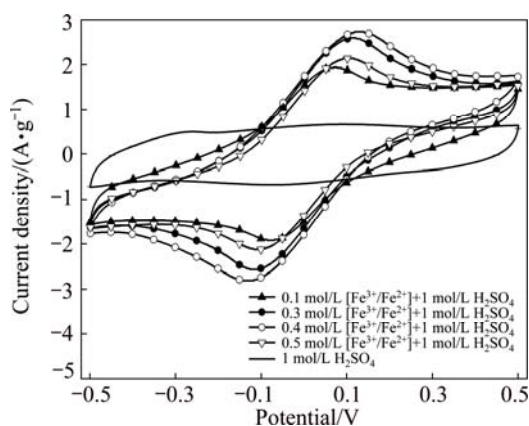


Fig. 1 CV curves at scan rate of 2 mV/s for PANI/SnO₂ supercapacitors

supercapacitors were recorded in 0.4 mol/L [Fe³⁺/Fe²⁺] + 1 mol/L H₂SO₄ electrolyte at various scan rates (2, 5, 10, 20, 50 mV/s) in the potential range of -0.5 to 0.5 V, as shown in Fig. 2. It can be seen from Fig. 2 that the supercapacitors exhibit similar curves as the scan rate increases. A couple of distinct redox peaks are observed and the reduction and oxidation potentials shift toward high and low potential sides, respectively, with increasing the scan rate. This kind of shifting may stem from the increased electrochemical polarization at an increasing scan rate [13,14].

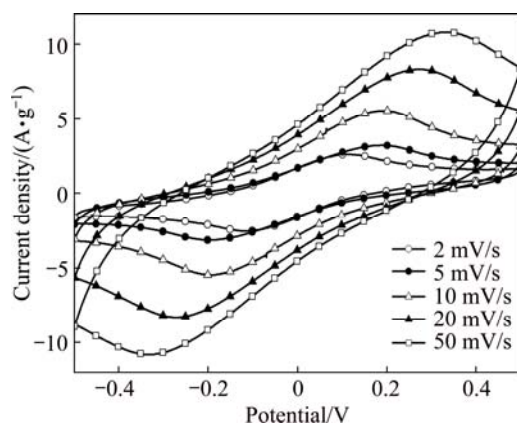


Fig. 2 CV curves at different scan rates for PANI/SnO₂ supercapacitors in 0.4 mol/L [Fe³⁺/Fe²⁺] + 1 mol/L H₂SO₄ electrolyte

GCD measurements were also used to test the performance of capacitors. The GCD curves of PANI/SnO₂ supercapacitors at a constant current density of 1 A/g are shown in Fig. 3. The GCD curve of the supercapacitors with 1 mol/L H₂SO₄ electrolyte is nearly linear symmetry. But the supercapacitor with *n* mol/L [Fe³⁺/Fe²⁺] + 1 mol/L H₂SO₄ electrolytes exhibit clear deviation from the ideal triangular shape. Such plateaus characteristics are known to be typical effects of pseudocapacitive contributions [15].

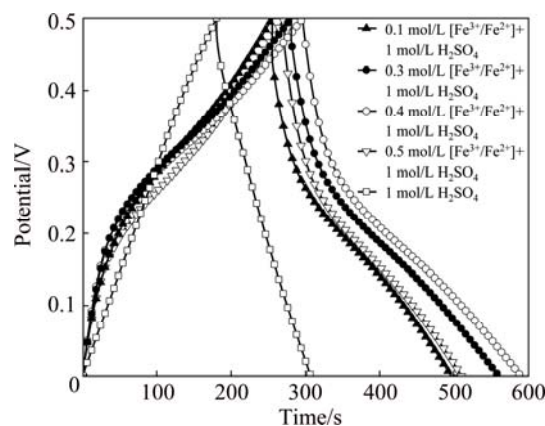


Fig. 3 GCD curves at 1 A/g for PANI/SnO₂ supercapacitors

The specific capacitance (*C*) of the electrode is evaluated from the GCD curves according to the following equation:

$$C = 2 \frac{I \times \Delta t}{\Delta V \times m} \quad (1)$$

where *I* is the discharge current (A), Δt is the discharge time (s), ΔV represents the voltage change during the corresponding discharge time (V), and *m* is the mass of the active material (g).

According to Eq. (1), the specific capacitances in four electrolytes change in the order of 1172 F/g (0.4 mol/L [Fe³⁺/Fe²⁺] + 1 mol/L H₂SO₄) > 1115 F/g (0.3 mol/L [Fe³⁺/Fe²⁺] + 1 mol/L H₂SO₄) > 963 F/g (0.5 mol/L [Fe³⁺/Fe²⁺] + 1 mol/L H₂SO₄) > 942 F/g (0.1 mol/L [Fe³⁺/Fe²⁺] + 1 mol/L H₂SO₄) > 525 F/g (1 mol/L H₂SO₄). Obviously, a significant improvement in the capacitive performance of the PANI/SnO₂ supercapacitor is achieved by using the [Fe³⁺/Fe²⁺] + H₂SO₄ electrolyte. The increase of capacitance is attributed to the additional pseudocapacitive contributions of reversible redox process of Fe³⁺/Fe²⁺.

The initial specific capacitances of the PANI/SnO₂ supercapacitors versus current densities in different Fe³⁺/Fe²⁺ concentrations (*n*) and in *n* mol/L [Fe³⁺/Fe²⁺] + 1 mol/L H₂SO₄ at different current densities are shown in Fig. 4. It further demonstrates that the specific capacitance values depend on the current densities (from 0.5 to 2 A/g) and Fe³⁺/Fe²⁺ concentrations for all the supercapacitors. It can be noted that the specific capacitance value of PANI/SnO₂ supercapacitor in 0.4 mol/L [Fe³⁺/Fe²⁺] + 1 mol/L H₂SO₄ electrolyte is much higher than those in other electrolytes, and the retention rate is more than 90% when the current density increases from 0.5 to 2 A/g. Consequently, the results obtained from GCD show that the PANI/SnO₂ supercapacitor in 0.4 mol/L [Fe³⁺/Fe²⁺] + 1 mol/L H₂SO₄ electrolyte performs good electrochemical reversible behavior and good rate capability.

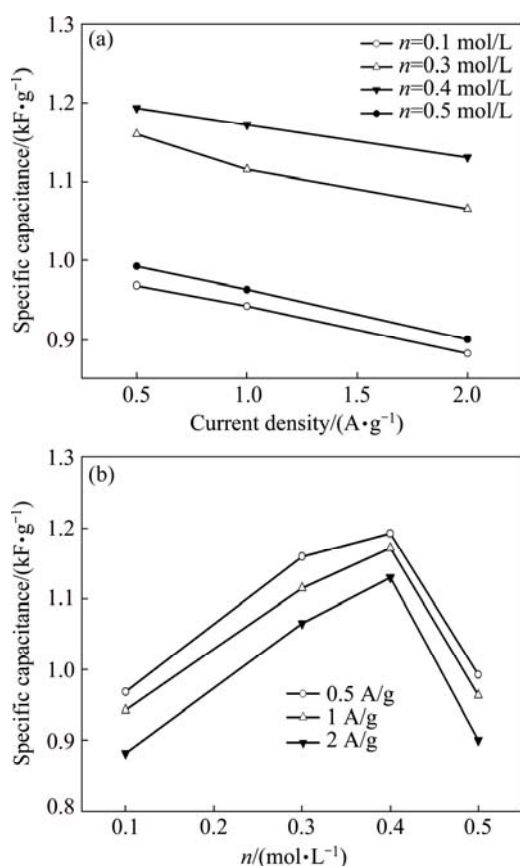


Fig. 4 Initial specific capacitances of PANI/SnO₂ supercapacitors vs current densities in different Fe³⁺/Fe²⁺ concentrations (n) (a) and in n mol/L [Fe³⁺/Fe²⁺]+1 mol/L H₂SO₄ at different current densities (b)

The long-term cycle stability of the PANI/SnO₂ supercapacitor using 0.4 mol/L [Fe³⁺/Fe²⁺] + 1 mol/L H₂SO₄ electrolyte was evaluated by repeating the GCD test at 1 A/g for 2000 cycles, as shown in Fig. 5. The specific capacitance falls at the beginning 500 cycles, after which the specific capacitance gradually increases and then reaches a constant of 1032 F/g. The specific capacitance increases with increasing the cycle number may be because the Fe³⁺/Fe²⁺ ions move from the bulk solution to the available surface and accumulate closer to the Helmholtz plane [16, 17]. These data further illustrate that Fe³⁺/Fe²⁺ redox electrolyte can be considered as promising electrolyte in the application of high-energy supercapacitor.

Figure 6 shows the EIS of PANI/SnO₂ supercapacitors measured in H₂SO₄ electrolyte with different Fe³⁺/Fe²⁺ concentrations. The first intersection point on the real axis of Nyquist spectrum in the high-frequency region reflected the Ohmic resistance of the electrolyte (R_s). The semicircle in the medium-frequency region is related with the interfacial charge transfer resistance (R_{ct}). The straight line in the low-frequency region is controlled by Warburg impedance [18]. As shown in Fig. 6, the straight line in four electrolytes is

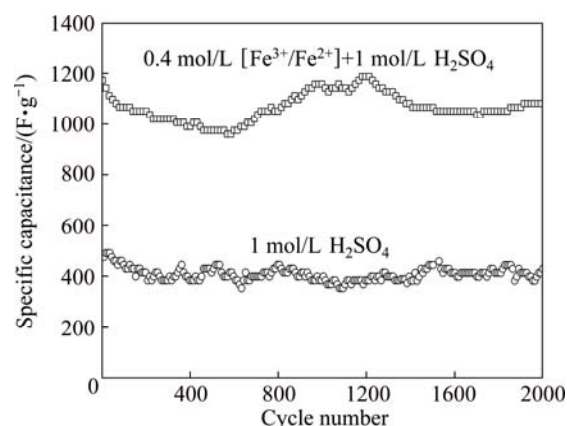


Fig. 5 Electrochemical cyclic stability of PANI/SnO₂ supercapacitors at 1 A/g

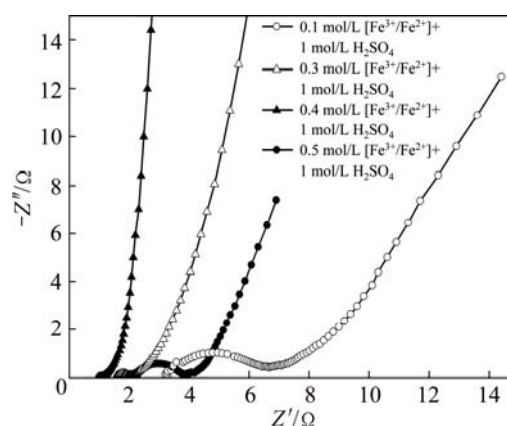


Fig. 6 EIS of PANI/SnO₂ supercapacitors

nearly parallel. The R_s , R_{ct} and capacitance values for PANI/SnO₂ supercapacitors in n mol/L [Fe³⁺/Fe²⁺]+1 mol/L H₂SO₄ are listed in Table 1. In diluted solution ($n=0.1$), the diffusion process is limited by the concentration of charged ions, which leads to low conductivity and large R_s value. As the electrolyte concentration increases, the amount of electrolyte ions rises. Thus, the ion transport will be easy which contributes to a high conductivity and low resistance of the system. However, if the electrolyte concentration is too high ($n=0.5$), the ion activity may be reduced due to the continuous accumulation of the electrolyte ions on the surface of the electrode. As shown in Table 1, the capacitance change exhibits an opposite trend to the changes of R_s and R_{ct} , and varies dramatically with the electrolyte concentration. These results are also well consistent with the results of CVs and GCD.

Table 1 R_s , R_{ct} and C for PANI/SnO₂ supercapacitors in n mol/L [Fe³⁺/Fe²⁺]+1 mol/L H₂SO₄ electrolyte

n	R_s/Ω	R_{ct}/Ω	$C/(F\cdot g^{-1})$
0.1	3.28	3.36	942
0.3	1.54	0.55	1115
0.4	0.95	0.1	1172
0.5	2.28	1.58	963

4 Conclusions

1) The PANI/SnO₂ supercapacitor fabricated using 0.4 mol/L [Fe³⁺/Fe²⁺] + 1 mol/L H₂SO₄ redox electrolyte gives a maximum capacitance of 1172 F/g at 1 A/g, which is higher than the corresponding values obtained using the conventional H₂SO₄ electrolyte and H₂SO₄ electrolyte doped by HQ.

2) The supercapacitor exhibits excellent long-term cyclability, with the specific capacitance decrease by 12% after 2000 cycles.

3) It is believed that Fe³⁺/Fe²⁺ redox electrolyte is an environmental friendly and high-efficient redox mediator compared with HQ redox electrolyte, and using Fe³⁺/Fe²⁺ redox electrolyte has a good prospect for improving the performances of energy-storage devices.

References

- [1] WU Chun, WANG Xian-you, ZHAO Qing-lan, GAO Jiao, BAI Yan-song, SHU Hong-bo. Effects of preparation temperature on electrochemical performance of nitrogen-enriched carbons [J]. Transactions of Nonferrous Metals Society of China, 2014, 24(11): 3541–3550.
- [2] DOU Yuan-yun, LUO Min, LIANG Sen, ZHANG Xue-ling, DING Xiao-yi, LIANG Bin. Flexible free-standing graphene-like film electrode for supercapacitors by electrophoretic deposition and electrochemical reduction [J]. Transactions of Nonferrous Metals Society of China, 2014, 24(5): 1425–1433.
- [3] MAO L, ZHANG K, CHAN H S O, WU J. Surfactant-stabilized graphene/polyaniline nanofiber composites for high performance supercapacitor electrode [J]. Journal of Materials Chemistry, 2012, 22(1): 80–85.
- [4] CHANNU V S R, HOLZE R. Synthesis and characterization of a polyaniline-modified SnO₂ nanocomposite [J]. Ionics, 2012, 18(5): 495–500.
- [5] ZOU Min-min, AI Deng-jun, LIU Kai-yu. Template synthesis of MnO₂/CNT nanocomposite and its application in rechargeable lithium batteries [J]. Transactions of Nonferrous Metals Society of China, 2011, 21(9): 2010–2014.
- [6] VONLANTHEN D, LAZAREV P, SEE K A, WUDL F, HEEGER A. A stable polyaniline–benzoquinone–hydroquinone supercapacitor [J]. Advanced Materials, 2014, 26(30): 5095–5100.
- [7] WU W, LI Y, YANG L, MA Y, PAN D, LI Y. A facile one-pot preparation of dialdehyde starch reduced graphene oxide/polyaniline composite for supercapacitors [J]. Electrochimica Acta, 2014, 139: 117–126.
- [8] HE S, WEI J, GUO F, XU R, LI C, CUI X, ZHU H, WU D. Flexible polyaniline/buckypaper composite with a core–shell structure for efficient supercapacitors [J]. Journal of Materials Chemistry A, 2014, 2(16): 5898–5902.
- [9] CAO Xue, SHU Yong-chun, HU Yong-neng, LI Guang-ping, LIU Chang. Integrated process of large-scale and size-controlled SnO₂ nanoparticles by hydrothermal method [J]. Transactions of Nonferrous Metals Society of China, 2013, 23(3): 725–730.
- [10] SELVAN R K, PERELSHTAIN I, PERKAS N, GEDANKEN A. Synthesis of hexagonal-shaped SnO₂ nanocrystals and SnO₂@C nanocomposites for electrochemical redox supercapacitors [J]. The Journal of Physical Chemistry C, 2008, 112(6): 1825–1830.
- [11] ROLDÁN S, GRANDA M, MENÉNDEZ R, SANTAMARÍA R, BLANCO C. Mechanisms of energy storage in carbon-based supercapacitors modified with a quinoid redox-active electrolyte [J]. The Journal of Physical Chemistry C, 2011, 115(35): 17606–17611.
- [12] ZHU Y, LIU E, LUO Z, HU T, LIU T, LI Z. A hydroquinone redox electrolyte for polyaniline/SnO₂ supercapacitors [J]. Electrochimica Acta, 2014, 118: 106–111.
- [13] LIM Y J, PARK M Y, LEE S K, LEE W K, JO N J. Polyaniline and multi-walled carbon nanotube composite electrode for rechargeable battery [J]. Transactions of Nonferrous Metals Society of China, 2012, 22(S3): s717–s721.
- [14] WANG Q, YAN J, FAN Z, WEI T, ZHANG M, JING X. Mesoporous polyaniline film on ultra-thin graphene sheets for high performance supercapacitors [J]. Journal of Power Sources, 2014, 247: 197–203.
- [15] WANG W, HAO Q, LEI W, XIA X, WANG X. Ternary nitrogen-doped graphene/nickel ferrite/polyaniline nanocomposites for high-performance supercapacitors [J]. Journal of Power Sources, 2014, 269: 250–259.
- [16] XIONG W, LIU M, GAN L, LV Y, LI Y, YANG L, XU Z, HAO Z, CHEN L. A novel synthesis of mesoporous carbon microspheres for supercapacitor electrodes [J]. Journal of Power Sources, 2011, 196(23): 10461–10464.
- [17] TIAN Y, YAN J, XUE R, YI B. Influence of electrolyte concentration and temperature on the capacitance of activated carbon [J]. Acta Physico-Chimica Sinica, 2011, 27(2): 479–485.
- [18] ZHANG X, WANG X, SU J, WANG X, JIANG L, WU H, WU C. The effects of surfactant template concentration on the supercapacitive behaviors of hierarchically porous carbons [J]. Journal of Power Sources, 2012, 199: 402–408.

Fe³⁺/Fe²⁺氧化还原电解液在 高性能聚苯胺/SnO₂ 超级电容器中的应用

刘田田, 朱银海, 刘恩辉, 罗珍玉, 胡添添, 李增鹏, 丁 锐

湘潭大学 化学学院, 环境友好化学与应用教育部重点实验室, 湘潭 411105

摘 要: 报道 Fe³⁺/Fe²⁺氧化还原电解液在聚苯胺/SnO₂ 超级电容器中的应用, 研究不同浓度的 Fe³⁺/Fe²⁺离子对与 1 mol/L H₂SO₄ 溶液组成的氧化还原电解液在超级电容器中的赝电容行为。用循环伏安法、恒电流充放电法和交流阻抗法对超级电容器的电化学性能进行研究。当 Fe³⁺/Fe²⁺浓度为 0.4 mol/L 时, 超级电容器的性能最好, 其在 1 A/g 电流密度下的比容量达到 1172 F/g。将聚苯胺/SnO₂ 超级电容器进行长期的循环实验, 经过充放电循环 2000 次后, 其起始容量保持率达到 88%。实验结果表明, 使用 Fe³⁺/Fe²⁺氧化还原电解液来提高能量储存装置的性能具有很好的前景。

关键词: 聚苯胺; 二氧化锡; 铁离子; 氧化还原电解液; 超级电容器

(Edited by Mu-lan QIN)